Vol. 723: 119–134, 2023
https://doi.org/10.3354/meps14265

MARINE ECOLOGY PROGRESS SERIES
Mar Ecol Prog Ser

Published November 23[§]

Contribution to the Theme Section 'Wind and weather effects on seabird foraging, movement and energetics'

Wind driven effects on the fine-scale flight behaviour of dynamic soaring wandering albatrosses

Stefan Schoombie[1,3,*], Rory P. Wilson[2], Peter G. Ryan[1]

[1]FitzPatrick Institute of African Ornithology, DST-NRF Centre of Excellence, University of Cape Town, Rondebosch, 7701, South Africa

[2]Department of Biosciences, Swansea University, Swansea SA1 8PP, UK

[3]*Present address:* Centre for Statistics in Ecology, Environment and Conservation (SEEC), Department of Statistical Sciences, University of Cape Town, 7701, South Africa

ABSTRACT: Wandering albatrosses *Diomedea exulans* are among the largest flying birds. Their energy-efficient dynamic soaring flight allows them to travel large distances by exploiting the gradient in wind strength above the sea surface. We used bio-logging devices to study the dynamic soaring flight behaviour of wandering albatrosses, deriving roll (bank) angles from video and tri-axial magnetometers, and flapping events from tri-axial accelerometers. Albatrosses mostly experienced westerly winds coming from their left during outbound flights from their colonies and from their right when returning. They compensated for differences in wind speed by varying their roll angles and predominantly turning into the wind, resulting in a net displacement that was perpendicular to the wind. Flapping flight was influenced by wind speed and direction, with birds spending more time flapping in light winds and in head winds. Flapping often occurred at the upper turn of the dynamic soaring cycle, a stage previously considered devoid of flapping. There was also evidence of sexual differences in flight behaviour, with females flapping less than males. Males almost exclusively take off into head winds, whereas females utilized cross winds as well. These results add to our knowledge of dynamic soaring and show how albatrosses react to their wind fields at a fine scale.

KEY WORDS: Bio-logging · *Diomedea exulans* · Seabird · Southern Ocean · Sub-Antarctic · Inertial measurement unit · IMU

1. INTRODUCTION

Wandering albatrosses *Diomedea exulans* are among the largest flying birds, and have the largest wingspan of extant birds (Tickell 2000). They can cover thousands of kilometres in a single foraging trip, making them one of the farthest ranging pelagic seabirds (Jouventin & Weimerskirch 1990, Weimerskirch & Wilson 2000, Mackley et al. 2010, Weimerskirch et al. 2012, 2014). This is achieved by undertaking long, multiday incubation and chick-provisioning trips, and spending up to 17 h in periods of flight (Weimerskirch et al. 1997, Mackley et al. 2010). In general, wandering albatrosses land less frequently than smaller albatrosses (Phalan et al. 2007). Breeding adults either forage throughout long looping trips or direct flights to specific foraging areas (Weimerskirch et al. 1997).

Like most procellariiform species, wandering albatross flight is largely influenced by wind, with birds utilizing dynamic soaring for low-energy flight (Pennycuick 1982, Weimerskirch et al. 2000, 2012, Sachs 2005, Richardson 2011, Sachs et al. 2012). The heart rates of flying wandering albatrosses are often only slightly elevated above resting rates, with lowest rates when ground speed is high (Weimerskirch et al. 2000). To achieve such energy efficient flight, wandering albatrosses minimize flapping and utilize gliding flight (Pennycuick 1982). Flapping flight is an expensive flight mode for large soaring birds (Aler-

*Corresponding author: schoombie@gmail.com

[§]Advance View was available April 13, 2023

Publisher: Inter-Research · www.int-res.com

stam et al. 1993, Weimerskirch et al. 2000, Williams et al. 2020a) and wandering albatrosses employ flight strategies that limit energy expensive take-offs, especially in light winds (Mackley et al. 2010). They are more prone to take-off when favourable wind conditions arise and adjust their flight patterns with changing wind conditions (Clay et al. 2020). Wandering albatrosses also vary their responses to wind depending on sex, where larger males (with greater wing loading) tend to forage farther south where wind speeds are on average greater (Weimerskirch et al. 2000). Female wandering albatrosses also take off in lighter winds than males, suggesting that males avoid landing in light winds where they might have increased energetic costs when taking off (Clay et al. 2020).

Over the past 2 decades, our knowledge of dynamic soaring flight has increased substantially, largely due to advances in bio-logging technology that have provided accurate, fine-scale (1–10 Hz) location estimates for extended periods of albatross flight (Weimerskirch et al. 2002, Sachs et al. 2012, 2013). Such data have shown that dynamic soaring consists of sequential cycles, of 10–15 s (Sachs 2005, Richardson 2011). The leeward turn is pivotal for dynamic soaring (Sachs et al. 2013), and upwind flight is possible through variations of tacking flight modes (Sachs 2016, Richardson et al. 2018). There is much debate regarding the exact means of energy gain from dynamic soaring (Richardson 2011, Sachs et al. 2012, 2013, Kempton et al. 2022), but flapping flight is usually excluded as a means of energy gain (Sachs et al. 2013).

Direct observations of flying albatrosses confirm that they seldom flap, but occasionally flap-glide in light winds (Pennycuick 1982, Spear & Ainley 1997, Richardson 2011). Initial studies using bird-borne heart rate monitors suggested that flapping flight in wandering albatrosses was mainly limited to take-off and landing events (Weimerskirch et al. 2000, Shaffer et al. 2001a). More recently, accelerometer data showed that albatrosses have 2 flapping modes, with greater flapping frequencies during take-off compared with cruising flight (Sato et al. 2009). These studies highlight the complexity of seabird flight, and how new technologies can improve our understanding of these processes. More recently, the use of inertial measurement units (IMUs; including accelerometers and magnetometers) have been extended from the study of marine mammals and penguins to include flying birds (Wilmers et al. 2015). These have mainly identified flapping flight (oscillations of the vertical accelerometer axis around 1 *g*; Gómez Laich et al. 2008, Shepard et al. 2008, Conners et al. 2021), but magnetometers also can be used to study body/wing angles of birds soaring in thermals (Williams et al. 2018, 2020a).

Although body angle (roll/bank angle) is often mentioned in dynamic soaring studies (Sachs 2005, Richardson 2011, Sachs et al. 2013, Kempton et al. 2022), the direct measurement of such angles is rare. A change in roll angle is an important aspect of the dynamic soaring process because it determines the rate at which the birds turn and consequently the direction in which they fly. Furthermore, it has been inferred that flapping is not part of dynamic soaring flight (Sachs et al. 2013), but flapping has not been explicitly quantified in conjunction with the dynamic soaring cycle. Here we used a multi-sensor approach to add to our knowledge of dynamic soaring flight, and demonstrate how albatrosses adapt their flight to variable wind patterns in the Southern Ocean. Specifically, we tested whether wandering albatrosses altered their body angles in response to varying winds during flight.

2. MATERIALS AND METHODS

2.1. Logger deployment

A variety of loggers were deployed on 33 wandering albatrosses breeding on Marion Island (46° 50′ S, 37° 50′ E) between 2016 and 2020. The devices included customised video loggers, Daily Dairy IMUs (Wildbyte Technologies) and GPS loggers (CatTraQ, Catnip Technologies; i-gotU GT-120, Mobile Action Technology). Most loggers (n = 25) were deployed using waterproof Tesa tape (Beiersdorf) on the central dorsal contour feathers in line with the body axis of the birds. For 8 individuals, the IMUs were attached below the tail with Tesa tape to 5 central tail feathers. GPS loggers (42 × 26 × 10 mm, 15.7 g) recorded location at 1 s to 60 min intervals, the video loggers (77 × 34 × 18 mm, 48 g) recorded high-definition video at 24 frames per second and the IMUs (30 × 25 × 10 mm, 26 g) recorded tri-axial accelerometer and magnetometer data at 40 Hz. Up to 3 devices were attached to each bird, with a combined maximum mass (including waterproofing and attachment tape) of ~130 g, which is much less than 3% of the mass of typical adult wandering albatrosses (~7000 g). IMUs deployed in 2017 had a small magnet in a silicone paddle attached to the casing of the logger, designed to estimate airspeed, but this interfered with our ability to measure roll angles (see Section 2.2.2).

2.2. Analysis

2.2.1. Data preparation

GPS loggers provided location estimates at intervals ranging from 1 s to 60 min but were sub-sampled to 60 min intervals to match the lowest sampling rate. Hourly GPS locations were deemed acceptable because they matched the temporal resolution of wind data; these GPS locations were linked to hourly wind data at 10 m a.s.l. from the European Centre for Medium Range Weather Forecasts ERA5 reanalysis dataset (Hersbach et al. 2018). The ERA5 dataset comprises zonal and meridional wind speed components at a spatial resolution of 0.25° (which equates to 27 km latitudinally and 16–23 km longitudinally within the range of the tracked birds). The wind speed components were used to calculate wind speed and direction using the uv2ds function in the R-package rWind (https://CRAN.R-project.org/web/package=rWind). Each GPS location was assigned to 3 relative wind conditions based on the difference between GPS course and wind direction: (1) ≤45° for tail winds; (2) between 45° and 135° for cross winds; and (3) ≥135° for head winds. GPS-derived data were temporally matched with the IMU data, using the closest location where exact matches were not possible. Metrics derived from the IMU loggers were averaged for each GPS-hour (i.e. individual track points) when comparisons were made with environmental variables. The video data were also temporally matched to the IMU data, and visual inspection of roll angles (from both IMU and video loggers) allowed for exact matching of the data at infrasecond (~0.1 s) resolution. In this study, we limited the data collected to in-flight data by visual inspection of the data using custom software (DDMT, Wildbyte Technologies, http://wildbytetechnologies.com/research.html). The dynamic soaring of albatross flight produces a repeated pattern in tri-axial magnetometer data during flight (Conners et al. 2021), which can be easily identified through visual inspection. To analyse the effect of wind on take-off events, the first 10 s of every flight was isolated. The total number of flaps (see Section 2.2.3) and mean instantaneous heading (derived from magnetometer data) during take-off was compared with the wind speed and direction at the nearest GPS location.

2.2.2. Dynamic soaring cycles

Roll angles (rotation around the longitudinal axis) were estimated from IMU and video logger data. Video data were analysed using custom software to automatically detect roll angles from the horizon (Schoombie et al. 2019), and roll angles also were estimated from magnetometer data (Schoombie 2021). The latter method uses a directional cosine matrix to rotate the reference magnetic field vector (World Magnetic Model; https://www.ngdc.noaa.gov/geomag/WMM/DoDWMM.shtml) around the measured magnetometer values to produce estimates of roll and yaw angles. This assumes that the pitch angle is zero, which was acceptable for our data, as video footage indicated that the pitch angle was negligible during most flights of wandering albatrosses. As indicated previously, accurate roll angles from magnetometer data could not be estimated during 2017 deployments because the windspeed paddle magnet interfered with the calibration of the magnetometer axes. However, the relative roll angles could still be used to estimate the shape of the dynamic soaring cycle. This was done by normalizing the roll angles and then identifying the turns in the dynamic soaring cycle: tail-mounted IMU loggers were not effective at estimating soaring cycles because tail movement is independent of body roll when birds turn with steep bank angles (Gillies et al. 2011). The roll angles were smoothed with a 1 s running mean to remove outliers. Peaks in roll angles were identified as points where the slope changed from positive to negative (right turn) or vice versa (left turn), where a right turn peak had to be followed by a left turn peak to be valid (Fig. 1). Peaks within 2 s of each other were disregarded as a typical dynamic soaring cycle generally lasts ~10 s (Richardson 2011, Sachs et al. 2012). The number of cycles per 1 min of flight was summed for each flight. Additionally, the accelerometer data from the IMU loggers were used to estimate the centripetal force experienced by the birds during flight. This was done by first calculating the vector sum of static body acceleration (VeSBA), where the static component of each of the 3 axes was calculated by applying a rolling mean of 2 s on each axis respectively and subtracting 1 *g* (Williams et al. 2015). The vector sum of the static components of an accelerometer should be 1 *g* because of gravity; VeSBA > 1 *g* indicated increased centripetal forces experienced by the birds.

2.2.3. Flap identification

Data from the tail-mounted loggers (n = 8) were excluded from the analysis of flapping flight as these loggers were not aligned with the birds' centre of

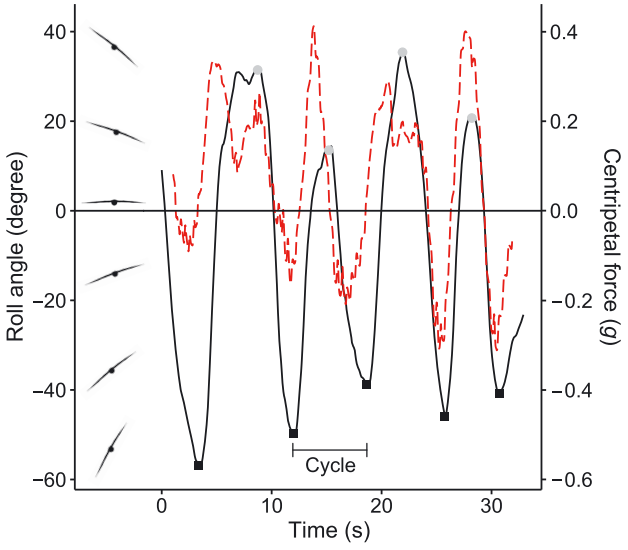

Fig. 1. Identification of dynamic soaring cycles from roll angles extracted from a video logger on a wandering albatross. Data between positive (grey circles: right turn) or negative (black squares: left turn) spikes are counted as individual dynamic soaring cycles. Red dashed line shows the centripetal acceleration (g) calculated from the accelerometer data

gravity. Flaps were identified as spikes in the heave (A_z) data. These spikes were isolated following Lotz & Clilverd (2019) using a type of band-pass filter (based on LULU operators) to isolate downward spikes within a range of bandwidths (k = lower limit, m = upper limit). This method identifies spikes purely based on the duration of the pulse, regardless of intensity. Spikes below a chosen threshold (th_{flap}) were subsequently labelled as flaps (Fig. 2), while ignoring spikes that were < m/2 apart. The th_{flap} value was chosen by plotting the total number of flaps isolated while incrementing th_{flap} by 0.1 g (range –2 to 0 g), while keeping k and m constant at 40 Hz (sampling frequency of IMUs) and 3 Hz (wandering albatross flapping frequency; Sato et al. 2009), respectively. Where the slope of the plots started levelling out (Fig. 3a), the corresponding th_{flap} was chosen for each individual bird. Next, the optimal m value was chosen for each individual as above, by incrementing m by 1 sample unit (range 1–20 sample units, i.e. 2–40 Hz) while keeping k at 1 sample unit (40 Hz) and th_{flap} at the value chosen in the previous step. Again, the m value that corresponded to the point where the slope started levelling out was chosen (Fig. 3b). Random sections of flight were visually inspected for each individual to see if the identified flaps seemed plausible. To estimate the time spent flapping, the flight data were rounded to 1-s intervals and each 1-s interval with at least one flap was labelled as *single flaps* while intervals with >2

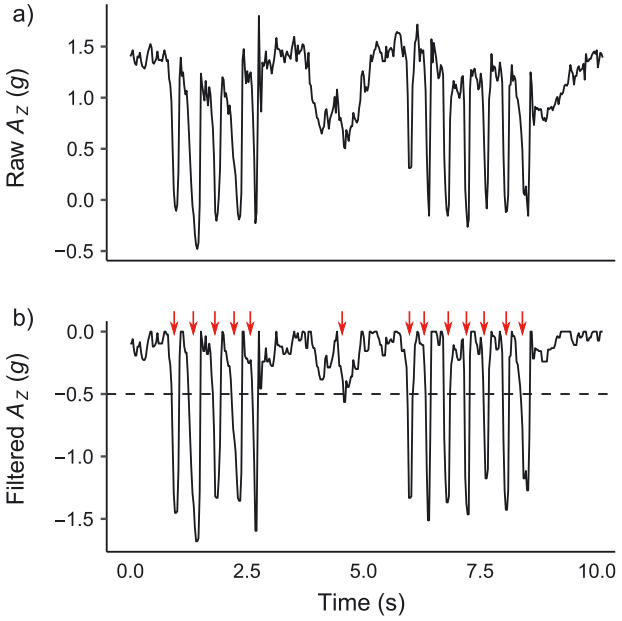

Fig. 2. Isolation of flaps (red arrows) from the vertical (heave) accelerometer axis (A_z) showing how the (a) raw data were (b) filtered; minimum values below a threshold (th_{flap}, dashed line) were used to identify individual flaps (red arrows). The upper limit (m) of the band-pass filter was set to 10

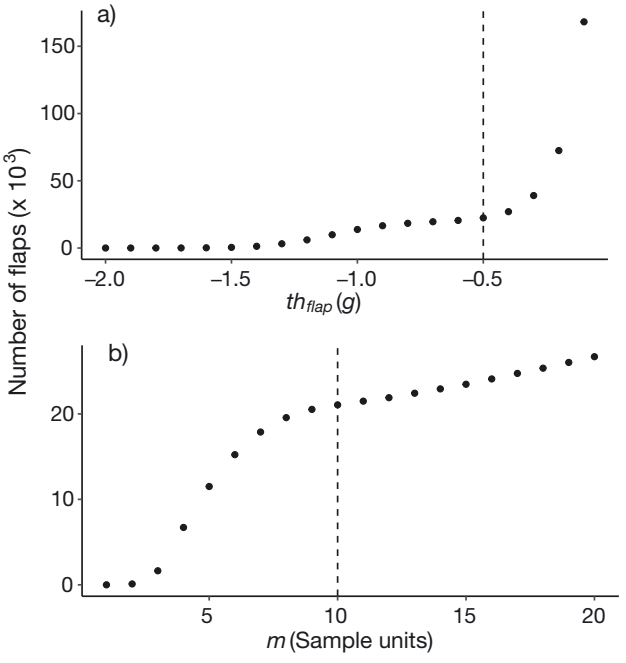

Fig. 3. Example of how parameters (a) th_{flap} (the threshold applied to peaks in accelerometer data) and (b) m (the bandwidth of peaks in accelerometer data) values were chosen for flap identification for an individual wandering albatross. The dashed lines represent the chosen value for each parameter. These values were chosen for each individual, and subsequently used to identify flaps from the accelerometer data (heave axis)

flaps were labelled as *sequential flaps*. These intervals were presented as percentages of the total flight duration. The vector sum of dynamic body acceleration (VeDBA) was used to estimate flapping intensity. The dynamic component of the accelerometer axes was calculated by subtracting the static component (see above) for each respective axis, before performing the vector sum (Qasem et al. 2012).

To test for significant differences in means (reported as mean ± SD unless otherwise stated) between groups, 2-sample *t*-tests were used, or Wilcoxon rank-sum tests were used when normality of the data could not be attained by standard transformations. A non-parametric generalised additive model (GAM) was used to show the relationship between flapping intensity and centripetal forces (*g*) as well as the relationship between flapping flight and wind speed. This was done using a penalised cubic regression spline with the smoother function *s* in the R package *mgcv* (Wood 2011). All statistical analyses were performed in the R software environment (version 4.2.0; R Core Team 2020).

3. RESULTS

All but one of the 33 loggers were retrieved with useful IMU data from 19 individuals (Table 1); the remaining 14 birds had devices that did not record any data or ran out of battery charge before the birds left their nests. All the valid IMU deployments had accompanying location data from GPS loggers and 8 individuals had overlapping video data during flight (Table 1).

A total of 624 flights were isolated from 1238 h of IMU data (694 h of flight data). Most IMU data (76%) and all the video footage were recorded during outbound sections of foraging trips. However, GPS tracks covered complete foraging trips for all but one bird (D2). The video loggers recorded 8.1 h of flight from 13 flights (8 birds) and all flying footage

Table 1. Summary of data recorded from 19 breeding wandering albatrosses on Marion Island between 2016 and 2020. Values are averages across flights per individual unless total values are stated

ID	Date	Sex	Video dur. (min)	Total dur. (h)	Total flights	Flights per day	Flight dur. (s)	Dynamic soaring			Flapping		Sequential flaps (% of flight)
								Cycles per min	Cycle dur. (s)	Flaps per min	Flapping intensity (*g*)	Single flap (% of flight)	
A1	2016-04-14	f	0	32	22	16	4485	7	8	15	0.88	16	2
A2[a]	2016-04-14	m	0	119	50	10	5367	–	–	–	–	–	–
A3[a]	2016-04-14	m	0	65	17	6	7609	–	–	–	–	–	–
A4	2016-04-15	m	0	93	24	6	8383	5	11	25	1.15	27	3
B1	2017-02-16	f	0	40	24	14	4457	6	8	21	0.75	22	3
B2	2017-03-16	f	17	46	25	13	3698	6	11	14	0.76	13	3
B3	2017-03-24	f	45	42	14	8	4233	5	13	8	0.81	8	1
B4	2017-03-23	m	0	6	7	–	576	8	7	65	0.88	57	13
B5	2017-04-08	m	12	44	35	19	2265	6	9	15	0.8	15	2
B6	2017-04-08	m	1	34	25	18	3891	7	8	15	0.89	15	2
C1[a]	2018-04-13	f	2	168	83	12	4128	–	–	–	–	–	–
C2[a]	2018-04-14	f	2	89	45	12	3393	–	–	–	–	–	–
C3	2018-04-15	f	0	36	26	17	4096	6	9	6	0.82	6	2
C4[a]	2018-04-15	f	0	146	48	8	6508	–	–	–	–	–	–
C5[a]	2018-04-13	m	0	71	50	17	3755	–	–	–	–	–	–
C6[a]	2018-04-13	m	0	46	37	19	2409	–	–	–	–	–	–
C7	2018-04-15	m	0	59	54	22	2926	6	9	29	0.85	26	5
D1	2020-03-13	f	202	35	14	10	4376	7	9	22	1.09	23	2
D2	2020-03-15	m	212	69	24	8	7545	6	10	14	0.93	15	2
	Mean ± SD				**33 ± 18**	**14 ± 6**	**4426 ± 1959**	**6 ± 1**	**9 ± 2**	**21 ± 15**	**0.88 ± 0.12**	**20 ± 13**	**3 ± 3**

[a]Tail-mounted devices

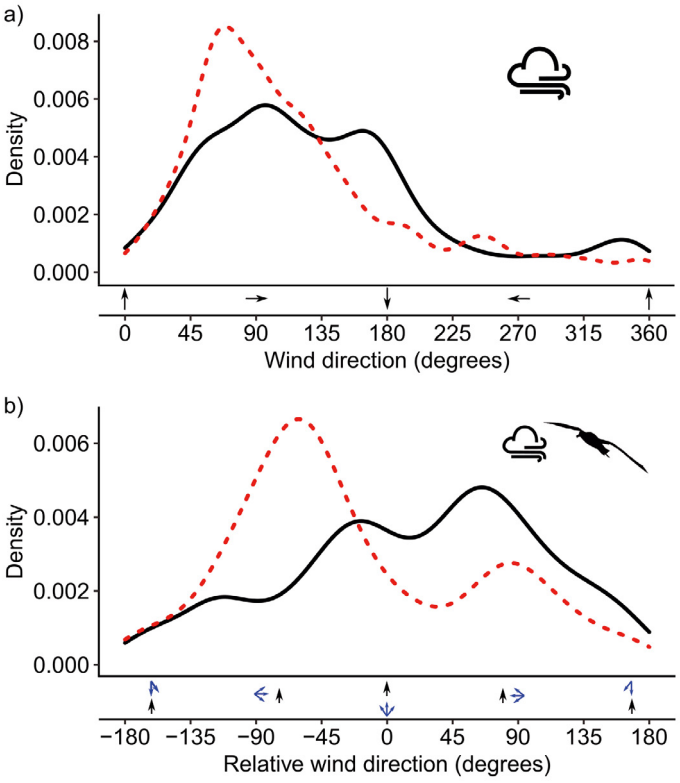

Fig. 4. Winds experienced by 32 wandering albatrosses. (a) Absolute wind direction where values are the direction towards which the wind is blowing (i.e. 0° is wind blowing to the north). (b) Difference between the bird's course over ground and the wind direction, so that negative values are winds coming from the left and positive values for winds from the right. Data for both outbound (red dashed lines) and inbound (solid black lines) sections of foraging trips are shown

recorded on the video loggers was correctly identified as flying periods from the matched IMU data (visual inspection). Birds performed 14 ± 6 flights per day (range 6–40) with an average duration of 1.2 ± 0.5 h (range 8 s to 12 h) per flight.

Wandering albatrosses predominantly experienced westerly winds during the study (Fig. A1 in the Appendix). However, more northerly winds were experienced during the inbound period of foraging trips, when birds returned to their colony (Fig. 4a). Wandering albatrosses flew mostly with cross winds (76%) from their left (outbound flights) and right (inbound flights), and tail winds (22%) during inbound flights (Fig. 4b). Flying birds experienced average wind speeds of 12 ± 5 m s^{-1} (range 1–25 m s^{-1}).

3.1. Dynamic soaring cycles

Roll angle analyses were only performed for 6 individuals with back mounted loggers without magnetic paddles (birds A1, A4, C3, C7, D1, and D2) or where video data were available. Dynamic soaring cycles estimated from the video-derived roll angles were compared with cycles from magnetometer-derived angles. Dynamic soaring cycles estimated from video data had a mean duration of 8.4 ± 1.6 s and frequency of 7 ± 2 cycles per minute (Table 2), and this was not significantly different from magnetometer-derived cycles (*t*-test, t_{26} = 1.84, p = 0.08 and Wilcoxon rank sum test, Z = 0.57, p = 0.57). The estimated centripetal forces (g) experienced by the birds were compared with the estimated roll angles. This proved to be an effective way to estimate the different periods of the dynamic soaring cycles (see Fig. 1). Centripetal forces (g) are expected to be greatest during the lowest altitude following the descent phase and least when the bird is at the upper turn (highest altitude). Wandering albatrosses had a mean roll angle of 25 ± 9° (range −109° to 89°) during flight and had greater roll angles (29 ± 8°) when turning with the wind (low g turns) as opposed to turning into the wind (25 ± 9°; Wilcoxon rank sum test Z = 5.39, p < 0.01). When flying in cross winds (the

Table 2. Comparison of wandering albatross dynamic soaring cycles estimated from video and inertial measurement unit (IMU) loggers

Bird ID	Flight section	Duration (min)	Total cycles		Cycles per min		Cycle duration (s)	
			Video	IMU	Video	IMU	Video	IMU
B2	1	17	115	118	7	7	9	9
B3	2	10	68	79	6	8	9	8
B3	3	19	133	142	7	8	8	8
B3	4	9	69	78	7	8	8	7
B5	1	2	19	14	8	6	7	9
B5	2	4	23	34	5	8	10	8
B5	3	5	26	41	6	9	10	7
B6	1	0.5	2	3	5	7	12	7
C1[a]	1	2	20	12	10	6	6	5
C1[a]	2	2	20	10	10	5	6	6
D1	1	158	1036	1002	7	6	9	9
D1	2	44	352	369	8	8	8	7
D2	1	212	1375	1454	6	7	9	9

[a]Tail-mounted devices

majority of flights), the roll angle distribution was skewed, with birds spending more time at angles turning into the wind (i.e. with the wind blowing onto the back of the birds; Fig. 5), which were consistent with the shallower roll angles. Birds flying with tail winds had a more uniform distribution of roll angles, while one individual filmed flying into a head wind showed a bimodal distribution of roll angles (Fig. 5). As expected, the distribution of roll angles was influenced by wind speed, with greater angles at higher wind speeds (Fig. 5).

3.2. Flapping behaviour

Identifying individual flaps was challenging and the number of flaps per minute, reported below, likely were overestimated due to the inclusion of erroneous 'low intensity' flaps. These 'low intensity' flaps were most likely attitude corrections as opposed to propulsive flaps. Individual flaps were isolated from back-mounted IMU loggers (n = 13). On average, wandering albatrosses performed 21 ± 15 flaps per minute of flight with the largest number occurring at the start and ends of flights (Fig. 6). These single flaps represented 21 ± 13% of flight time, but sequential flapping (>2 flaps s^{-1}) only represented 3 ± 4% of the time. Likewise, averaging over individual flights could skew the data towards shorter flights where flapping is likely more pronounced, and the flapping rate was lower when averaged over hourly periods of flight compared with averages over complete flights. Most flaps occurred during periods with lesser centripetal acceleration

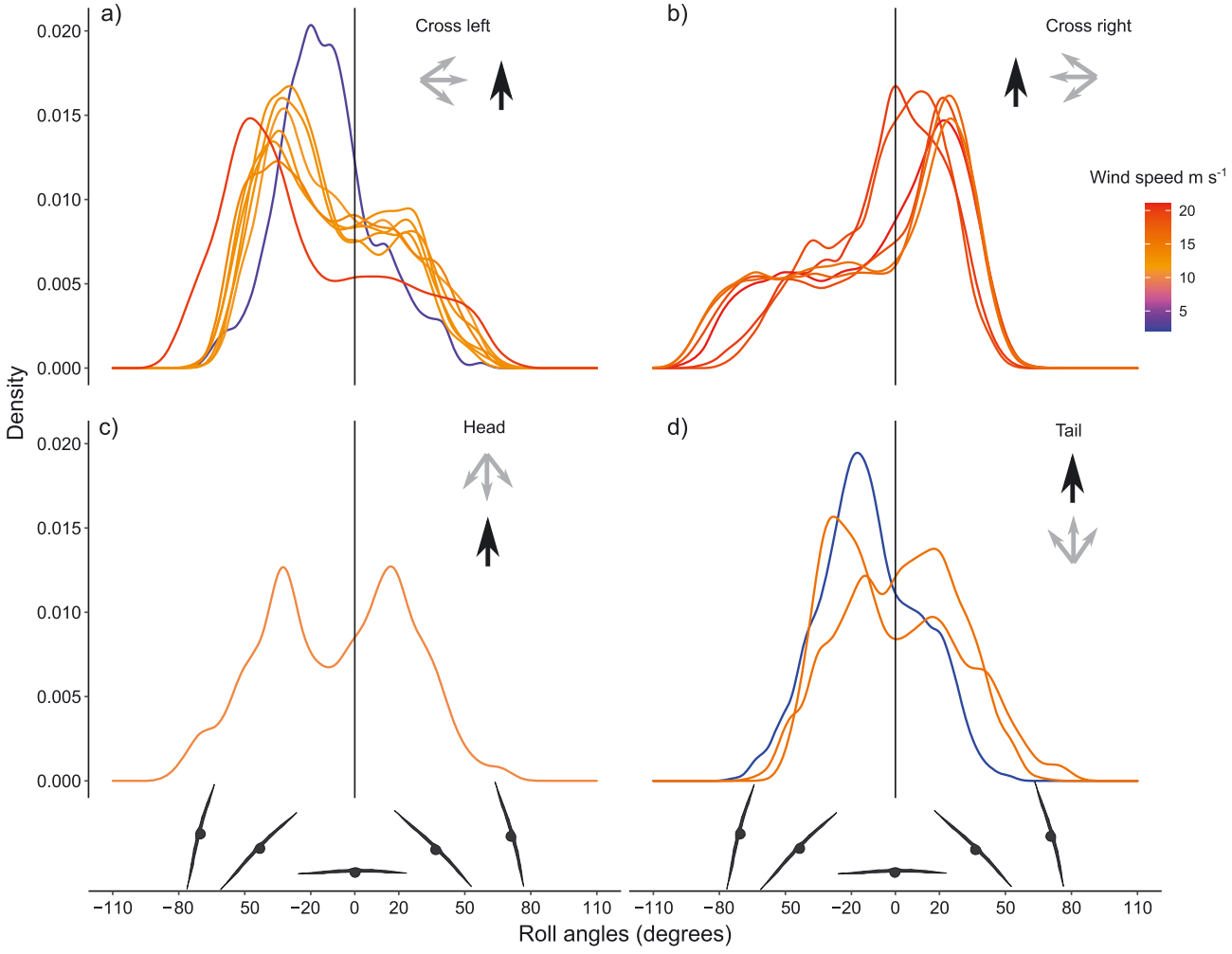

Fig. 5. Frequency distribution of roll angles extracted from video loggers on wandering albatrosses in relation to wind speed and wind direction (grey arrows) relative to flight direction (black arrow). The relative wind direction was grouped into 4 categories: (a) cross wind coming from the left, (b) cross wind coming from the right, (c) head wind, and (d) tail wind

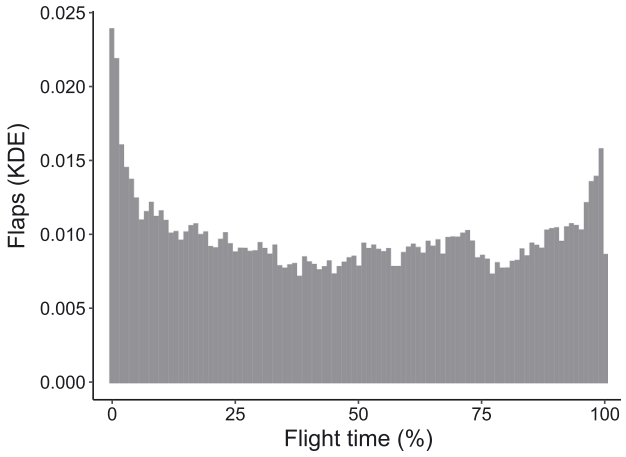

Fig. 6. Kernel density estimate (KDE) histogram of the number of flaps through the course of individual flights of wandering albatrosses

(*g*), which corresponded to the upper turn and the leeward descent of the dynamic soaring cycle (see Fig. 1 and Supplementary Videos S1 & S2 at www.int-res.com/articles/suppl/m723p119_supp/ for examples of wandering albatross flapping behaviour). The mean VeDBA (representing intensity) of flaps was 0.68 ± 0.28 *g* with a decreasing trend in VeDBA as centripetal acceleration increased (Fig. 7). Flapping intensity was not significantly different between sexes (male: 0.68 ± 0.09 *g*, female: 0.74 ± 0.13 *g*; t_9 = 0.92, p = 0.38) and was not different when restricted to take-off periods (0.86 ± 0.13 *g*; t_{10} = 10.0, p = 0.95). However, males had significantly greater flapping intensities during take-off (0.86 ± 0.14 *g*) than during sustained flight (0.68 ± 0.09 *g*; t_8 = 2.58, p = 0.03).

Wandering albatrosses were more likely to flap when flying in low wind speeds, with the highest frequency of flapping occurring during head winds (Fig. 8). Interestingly, the amount of flapping seemingly increased again at the highest wind speeds for cross and head winds, but this was only the case for 'low intensity' flaps (Fig. 8). The birds were able to fly in lower wind speeds without flapping when flying with tail winds, which had less flapping in general (Fig. 8). Males flapped more often (27 ± 18 flaps min^{-1}) than females (14 ± 7 flaps min^{-1}), but this was not statistically significant (Welch 2 sample *t*-test, t_{11} = 2.134, p = 0.056), likely due to the modest sample size. Whereas, males mostly took-off into headwinds, females took-off into both head and cross winds (Fig. 9a). Lower wind speeds resulted in more flapping during take-off, with males also flapping marginally more than females (Fig. 9b). One male wandering albatross flew into the wind for ~1 h flapping almost every second of the flight (54 flaps min^{-1}). This was just before the bird reached its maximum distance from Marion Island, where it spent ~12 h presumably foraging, before returning to the island.

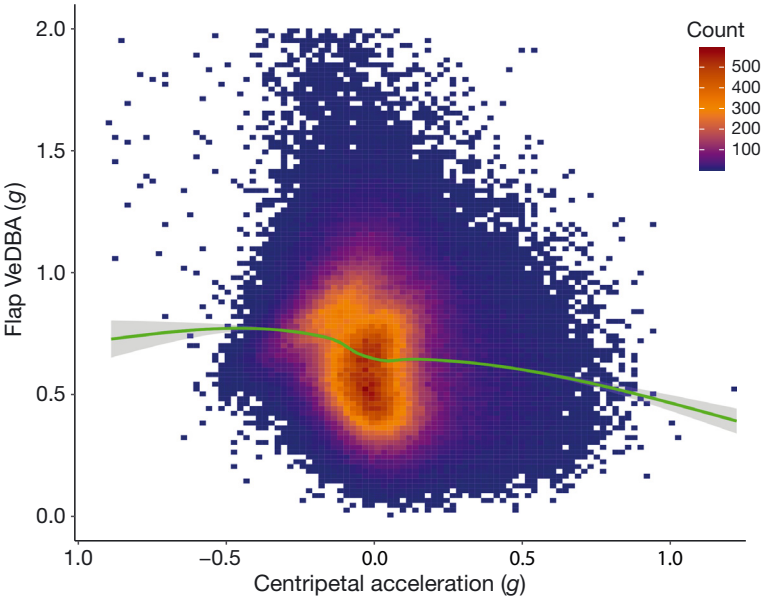

Fig. 7. 2D Density plot showing the relationship between centripetal acceleration and flapping intensity (VeDBA) for wandering albatross flapping flight. A generalised additive model (GAM) curve is shown as a green line with 95% CI (shaded grey)

A detailed illustration of the above results is shown in Fig. 10 and Supplementary Video S2, which show the outbound section of a foraging trip by wandering albatross D1. This female headed northwest into the wind, while frequently flapping at a high intensity (flight 7a; Fig. 10). As the northwesterly wind speed increased, the bird flapped less (flaps with very low intensity) and had more extreme roll angles when turning with the wind, resulting in the bird heading west (flight 7b; Fig. 10). When the wind speed decreased (flight 11; Fig. 10), the amount of flapping and flapping intensity increased, while the roll angles were less extreme. The wind then turned, coming from the southwest, resulting in the bird rolling towards the left (into the wind) more often and heading north-northwest while flapping infrequently. Supplementary Video S3 shows the flight behaviour of all tracked individuals in relation to wind.

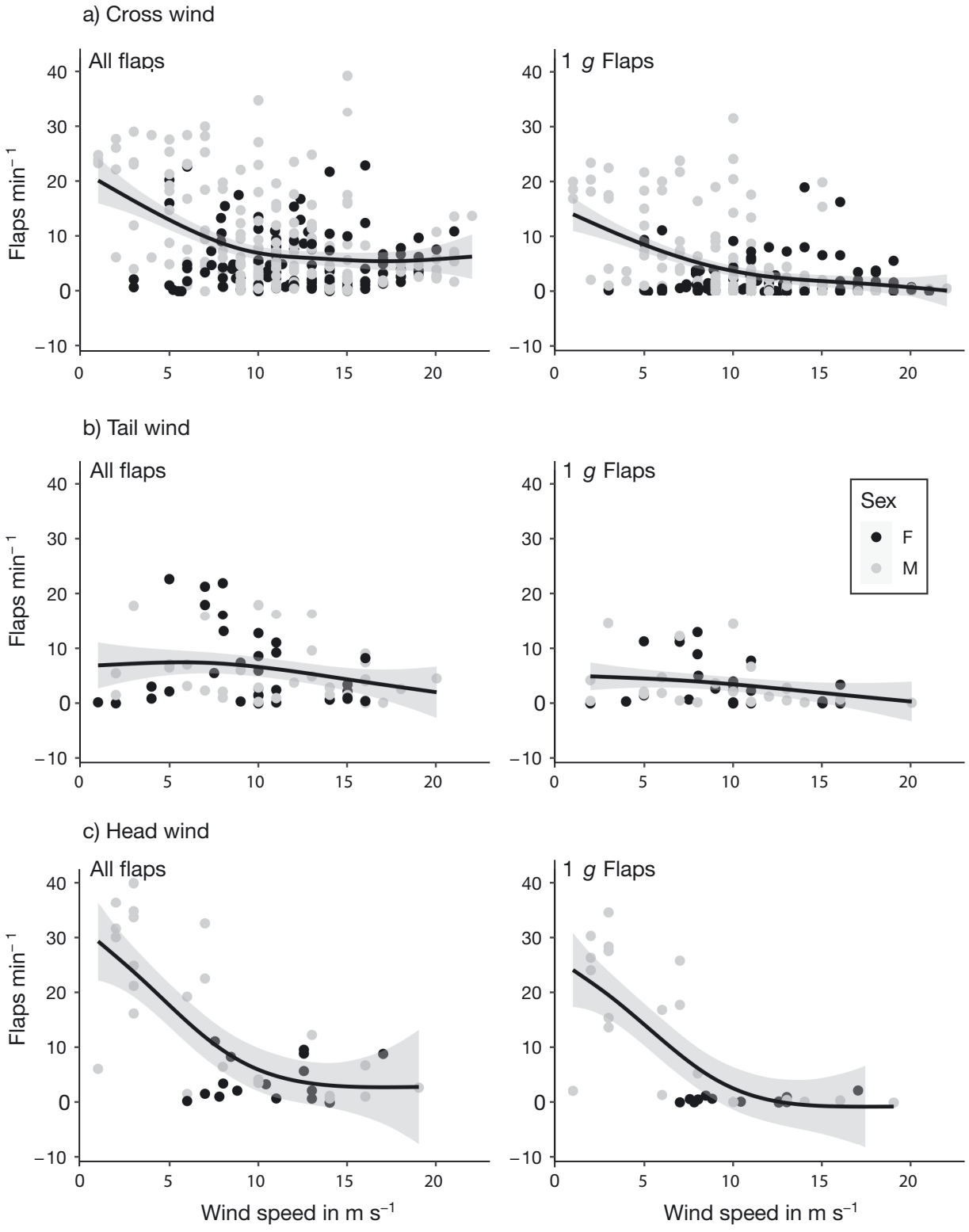

Fig. 8. Relationship of flapping flight and wind speed for wandering albatrosses flying with (a) cross winds, (b) tail winds, and (c) head winds. Left column: results for all flaps as identified by the chosen th_{flap} value (see Section 2.2.3); right column: results for 'high intensity flaps' where the flap intensity was >1 *g*. Generalised additive model (GAM) curves show trends for both sexes, with 95% CI in grey shading

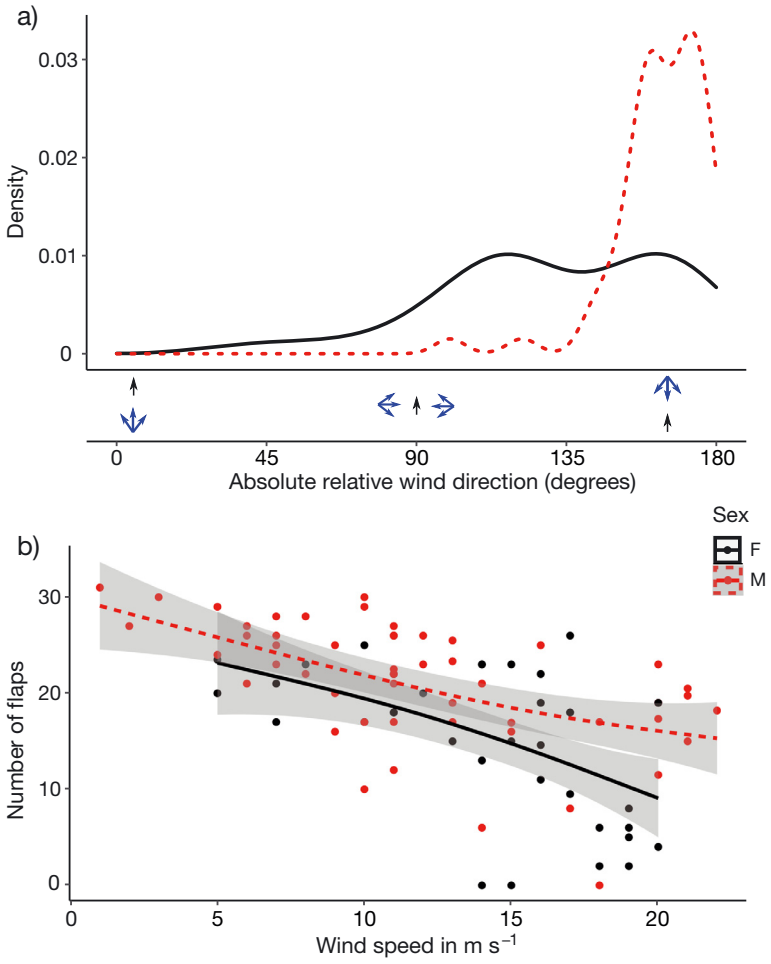

Fig. 9. Effect of wind direction and speed on the take-off behaviour of wandering albatross females (black solid lines) and males (red dashed lines), shaded areas are 95% CI. (a) Kernel density estimate of take-off heading relative to the wind direction experienced by the birds; (b) a generalised additive model (GAM) of the number of flaps occurring at varying wind speeds. Take-off periods were regarded as the first 10 s of individual flights

4. DISCUSSION

This is the first study to directly measure the fine-scale body angles of wandering albatrosses during dynamic soaring. Rapidly advancing bio-logging technology and new analytical tools have revolutionised ecological research (Rutz & Hays 2009, Williams et al. 2020b). In this study, we used a range of loggers to show how wandering albatrosses use dynamic soaring throughout waters surrounding Marion Island, one of the most consistently windy areas on Earth (le Roux 2008). Our results show how male and female albatrosses differ in their flight behaviour, possibly influencing their spatial distribution.

The average number of flights per day (14 ± 6) was similar to values from a previous study of wandering albatross activity (~14 flights per day; Weimerskirch et al. 2000). The distribution of flight durations was similar for both sexes, with both males and females flying for up to 12 h at a time. An appreciable proportion of flights (6% or n = 41) lasted <30 s. Video footage showed that some of these flights were during foraging events, but visual inspection of IMU data indicated that some might be failed take-off events, when a bird had been sitting for some time, then attempted to take-off repeatedly before the start of a long flight. Weimerskirch et al. (2000) measured an increased heart rate prior to take-off and hypothesised that this could be an anticipatory response. However, our data show that this increase in heart rate might also be due to failed take-off events.

Dynamic soaring cycles were identified from roll angle estimates, even when the absolute roll angles had a large error (due to magnetic interference caused by a magnetic paddle in deployments in 2017). Such magnetic interferences caused a shift in the roll angle estimates, but the general shape of the cycle was maintained. By normalizing the roll angles to a range of −1 to 1, the cycles could still be identified, and durations estimated. Unsurprisingly, data from tail-mounted loggers could not be used to estimate roll angles or dynamic soaring cycles because these loggers were not in line with the birds' centre of gravity, and because the tail may be angled independent of the body when turning. Roll angles from tail-mounted loggers could provide information on how tail movement responds to sudden changes in the wind, but this would need further validation (e.g. back facing cameras). The dynamic soaring cycles of wandering albatrosses lasted ~9 s, which is similar to estimates from fine-scale tracking data (~10 s; Sachs et al. 2013). By coupling the centripetal force (estimated from accelerometer data) to the estimates of roll angles, the windward and leeward turns of the dynamic soaring cycle could be identified, assuming that these forces peak during the descent phase of the cycle while the birds are turning into the wind.

Roll angle distribution during wandering albatross flight changed with wind conditions, and individuals

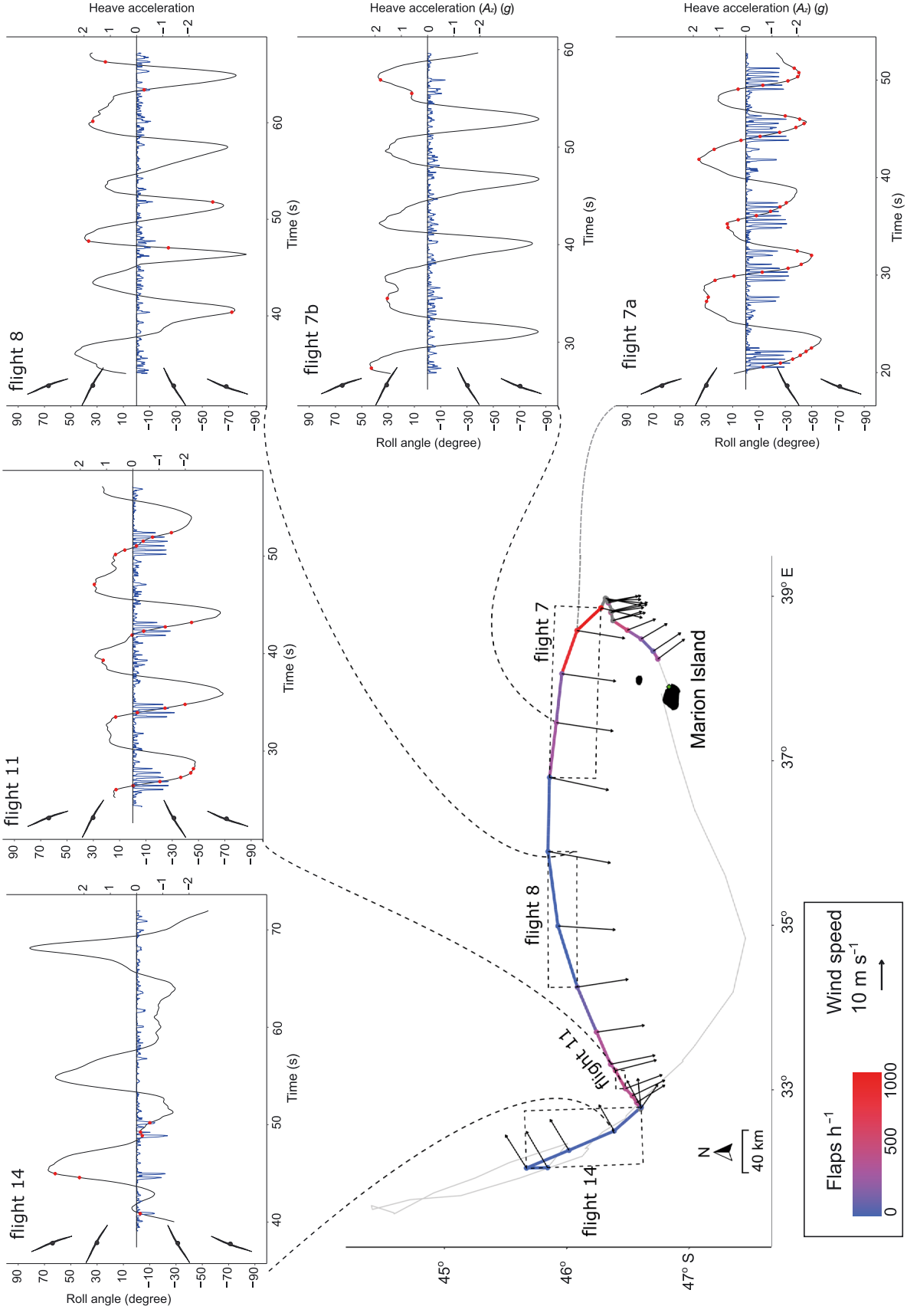

Fig. 10. Example of the flight behaviour of a female wandering albatross (bird D1) flying in varying wind conditions. Points are hourly GPS locations with colour representing the number of flaps for every location where inertial measurement unit (IMU) data were available (grey sections: IMU data were not available). Wind vectors are also shown for locations with IMU data while the remaining track is shown as a thin grey line. Inserts (based on dashed boxes around GPS points) are 30 s extracts of data from individual flights (i.e. data between take-off and landing events) showing roll angles (black) and the vertical accelerometer axis (A_z; blue) with individual flaps indicated by red dots in relation to the roll angles. Note that 2 flight segments are shown for flight 7 to illustrate different flight strategies. An accompanying video is shown in Supplementary Video S2 at www.int-res.com/articles/suppl/m723p119_supp/

often maintained a heading perpendicular to the wind by predominantly banking in the direction from which the wind was coming. Albatrosses and petrels tend to favour cross winds in the Southern Ocean (Sachs 2005, Nevitt et al. 2008, Weimerskirch et al. 2014, Tarroux et al. 2016) because these winds are seemingly predictable to the birds (Weimerskirch et al. 2000) and allow flight with minimal energy expenditure (Sachs et al. 2012). Flying with a cross wind can result in windward drift and birds must either compensate or tolerate such drift when trying to maintain a specific heading. We note that Antarctic petrels *Thalassoica antarctica* might be able to compensate for drift, but are apparently not always able to detect how much they are drifting (Tarroux et al. 2016). Our results indicated that wandering albatrosses may compensate for wind drift by altering their roll angle in response to changing wind conditions. The ability to compensate in this manner is probably influenced in part by body size. Male wandering albatrosses average 20% heavier than females with ~7% more wing area, and thus have 12% greater wing loading (Shaffer et al. 2001b), allowing them to fly with faster airspeeds in stronger winds, where the aerodynamic forces on the birds are greater (Richardson 2011). Most of the IMU and video data were recorded during the outbound period of foraging trips dominated by westerly winds. During these flights, wandering albatrosses were flying with the wind coming from their left and spent more time turning into the wind (left turn) and less time with the wind (right turn). By turning into the wind for longer periods, their net displacement was more or less perpendicular to the wind and resulted in a northerly bearing. The shape of the upper turn of the dynamic soaring cycle is likely to be relatively constant (Sachs 2016), thus the birds probably bank towards the left during the leeward descent, causing a net displacement perpendicular to the wind. Inbound sections of flight were dominated by northerly and westerly winds and the birds mostly flew with the wind coming from the right or from behind.

Flapping has not been explicitly regarded as being part of the dynamic soaring cycle and the exact means of energy gain from the cycle remains contentious (Richardson 2011, 2015, Sachs et al. 2012, 2013, Sachs 2016). This debate is particularly relevant to the design of unmanned aerial vehicles (UAVs) to travel across the ocean in the absence of powered flight, where upwind flight is of particular concern (Richardson 2015, Sachs 2016). Our results show one male wandering albatross flew for an extended period (~1 h) against the wind while flapping at a high rate (54 flaps min^{-1}). Flapping behaviour (deduced using the accelerometer data) occurred during periods of low centripetal acceleration, which was often associated with the upper turn of the dynamic soaring cycle, as identified by roll angles at lower *g* values (see Figs 1, 7 & 10). The upper turn of the dynamic soaring cycles is hypothesised to be where energy gain takes place, independent of flapping flight (Sachs et al. 2013, Sachs 2016). We suggest that this may not always be the case. Instead, wandering albatrosses might supplement dynamic soaring and energy gain during flight by flapping, especially when flying in light winds. As expected, the amount of flapping was greatest during take-off and landing (Weimerskirch et al. 2000). However, there was appreciable flapping during cruising flight, with ~3% of all flights consisting of continuous flapping (> 2 flaps s^{-1}). Sato et al. (2009) reported wandering albatrosses spent between 1.2 and 14.5% of their time flapping based on accelerometer data. Smaller black-browed albatrosses *Thalassarche melanophris* spend ~4% of their time flapping, amounting to 14% of their total energy expenditure during flight (Sakamoto et al. 2013).

Sato et al. (2009) inferred that albatrosses and petrels have 2 modes of flapping, a high frequency flap during take-off and a low frequency flap during cruising flight. We found that flapping intensity also varied with the stage of the dynamic soaring cycle. Higher intensity flapping occurred at low centripetal acceleration values (upper turn of the dynamic soaring cycle) while intensity decreased with increasing centripetal acceleration (lower turn). The latter were normally sporadic flaps during flights with low flapping percentages (see Fig. 10) and their lower intensity was expected presumably because the airspeed was greater, reducing gains of flaps and increasing the effort required to flap. Wing morphing (the flexing of wings) is important for stabilisation of seabirds in flight, especially when experiencing high wind speeds or gusts (Harvey et al. 2019). The low intensity flaps observed in wandering albatrosses might be wing morphing events for stability rather than power generating flaps, but this requires further investigation. Another explanation for these low intensity movements could be minor attitude corrections that the birds undergo to avoid the sea surface when flying close to the water.

As expected, the time spent flapping increased at lower wind speeds when the birds were flying with cross winds, but minimal flapping was required when flying in low tail winds. In the absence of wind, albatrosses may utilize updrafts caused by large

waves to perform a type of wave-slope soaring (Pennycuick 1982, Richardson 2011). With a tail wind, the birds could travel perpendicular to the waves and possibly supplement dynamic soaring flight with wave-slope soaring where wind speeds do not allow continuous dynamic soaring without flapping (Richardson 2011). Wandering albatrosses seldom fly into head winds, and sample sizes were too small to obtain clear results. However, males almost exclusively flew into the wind during take-off, whereas females took off into cross winds and head winds. Flapping intensity (as manifest by VeDBA) was significantly greater during take-off than during sustained flight for male wandering albatrosses. Although not explicitly tested for albatrosses, dynamic acceleration metrics have shown promise as indicators of energy expenditure during flapping flight (Van Walsum et al. 2020). Take-off events in large soaring birds are seemingly the most energy expensive part of the flight (Weimerskirch et al. 2000, Williams et al. 2020a), so male wandering albatrosses might limit their take-offs to favourable wind conditions (Clay et al. 2020) and once airborne may increase flapping rather than landing when wind conditions become temporarily unfavourable. Taking off in favourable wind conditions may not be restricted to albatrosses, as this behaviour has also been observed for smaller seabird species (Kogure et al. 2016).

Although the small sample size rendered the result statistically non-significant, female wandering albatrosses also tended to flap less than males. Female wandering albatrosses are adapted to fly in lower winds than males (Shaffer et al. 2001b) because they are smaller (~20%) and have lower wing loadings, resulting in slower stall speeds (Warham 1977). Female wandering albatrosses from the Crozet archipelago and South Georgia are more likely than males to take-off in lower wind speeds and males fly in greater wind speeds than females (Clay et al. 2020). Birds from Marion Island (present study) flew in similar wind conditions regardless of sex during the breeding period, similar to a previous study of wandering albatrosses from South Georgia (Wakefield et al. 2009). Female wandering albatrosses from the Crozet archipelago (neighbouring Marion Island) are spatially segregated from males during the breeding period, as is the case during the non-breeding period but to a lesser extent (Weimerskirch et al. 2014). Although the data we collected were mostly during the brood-guard period (when foraging trips are short), and during outbound sections of flight, we found some evidence of sexual differences. Females flapped less and were seemingly more tolerant of low wind speeds. This could explain the affinity of males for higher wind speeds (Clay et al. 2020), because birds that are unable to take-off in low wind conditions likely have reduced foraging efficiency (Jouventin & Weimerskirch 1990). Flying in higher wind speeds could result in a larger degree of wind drift, and coupled with increased flight speeds could result in the wider distribution of males during the breeding period (Weimerskirch et al. 2014).

5. CONCLUSIONS

Our study demonstrated how multiple sensor biologging was used to infer fine-scale patterns in seabird flight behaviour. Although we used a visual approach to identify periods of flight because we had a modest sample size, future studies may benefit from automated methods, such as machine learning classifiers, for larger data sets (e.g. Conners et al. 2021). We showed how wind drives the flight behaviour of wandering albatrosses and how they reacted to wind conditions by altering roll angles. We also showed that flapping flight was present during most flights, and how this might be a key part of the dynamic soaring cycle when wind conditions present challenges. Future studies could add to these results using additional loggers, such as gyroscopes or side-facing cameras, to further study albatross flapping behaviour. One drawback of fine-scale studies, however, is the lack of matching fine-scale environmental data. How a dynamic soaring seabird's behaviour changes in response to fine-scale wind patterns is difficult to study with relatively coarse environmental data. Future studies, incorporating accurate measures of bird airspeed, might help to answer some of these questions (Williams et al. 2020b). Likewise, most of the GPS location data used in our study were relatively coarse (only 2 individuals with 1 Hz GPS data) and finer-scale location data could benefit future studies that address body angles and flapping behaviour. Fine-scale positional data could also potentially be used to estimate ocean winds (Yonehara et al. 2016), which would aid in the estimation of bird airspeed. It is likely that wandering albatrosses are also physically limited with regards to their roll angles when flying in high wind speeds, and research into their mechanical limits could also help to understand their behaviour. Lastly, we showed that Marion Island wandering albatrosses displayed sexual differences in flight behaviour and responses to changing wind speed conditions; together with our

results, study of more individuals in the future might help inform on the consequences of an increasingly windy Southern Ocean (le Roux 2008, Weimerskirch et al. 2012).

Acknowledgements. We thank all field assistants who helped with deployment and retrievals on Marion Island during the study period. The South African Department of Environmental Affairs provided logistic support on Marion Islands. Funding was provided by the FitzPatrick Institute of African Ornithology Centre of Excellence and the South African National Antarctic Programme, through the South African National Research Foundation. Permission to work on seabirds at the Prince Edward Islands was granted by the Prince Edward Islands' Management Committee. All research was approved by the University of Cape Town's Science Faculty Animal Ethics Committee (2017/V10REV/PRyan). We thank 2 anonymous reviewers whose comments improved a previous version of this manuscript.

LITERATURE CITED

Alerstam T, Gudmundsson GA, Larsson B (1993) Flight tracks and speeds of Antarctic and Atlantic seabirds: radar and optical measurements. Philos Trans R Soc Lond B Biol Sci 340:55–67

Clay TA, Joo R, Weimerskirch H, Phillips RA and others (2020) Sex-specific effects of wind on the flight decisions of a sexually dimorphic soaring bird. J Anim Ecol 89: 1811–1823

Conners MG, Michelot T, Heywood EI, Orben RA and others (2021) Hidden Markov models identify major movement modes in accelerometer and magnetometer data from four albatross species. Mov Ecol 9:7

Gillies JA, Thomas ALR, Taylor GK (2011) Soaring and manoeuvring flight of a steppe eagle *Aquila nipalensis.* J Avian Biol 42:377–386

Gómez Laich A, Wilson RP, Quintana F, Shepard ELC (2008) Identification of imperial cormorant *Phalacrocorax atriceps* behaviour using accelerometers. Endang Species Res 10:29–37

Harvey C, Baliga VB, Lavoie P, Altshuler DL (2019) Wing morphing allows gulls to modulate static pitch stability during gliding. J R Soc Interface 16:20180641

Hersbach H, Bell B, Berrisford P, Biavati G and others (2018) ERA5 hourly data on pressure levels from 1979 to present. Copernicus Climate Change Service (C3S) Climate Data Store (CDS)

Jouventin P, Weimerskirch H (1990) Satellite tracking of wandering albatrosses. Nature 343:746–748

Kempton JA, Wynn J, Bond S, Evry J and others (2022) Optimization of dynamic soaring in a flap-gliding seabird and its impacts on large-scale distribution at sea. Sci Adv 8: eabo0200

Kogure Y, Sato K, Watanuki Y, Wanless S, Daunt F (2016) European shags optimize their flight behavior according to wind conditions. J Exp Biol 219:311–318

le Roux P (2008) Climate and Climate Change. In: Chown SL, Froneman PW (eds) The Prince Edward Islands: land-sea interactions in a changing ecosystem. Stellenbosch University Press, Stellenbosch, p 39–64

Lotz SI, Clilverd M (2019) Demonstrating the use of a class of min–max smoothers for D region event detection in narrow band VLF phase. Radio Sci 54:233–244

Mackley EK, Phillips RA, Silk JRD, Wakefield ED, Afanasyev V, Fox JW, Furness RW (2010) Free as a bird? Activity patterns of albatrosses during the nonbreeding period. Mar Ecol Prog Ser 406:291–303

Nevitt GA, Losekoot M, Weimerskirch H (2008) Evidence for olfactory search in wandering albatross, *Diomedea exulans.* Proc Natl Acad Sci USA 105:4576–4581

Pennycuick CJ (1982) The flight of petrels and albatrosses (Procellariiformes), observed in South Georgia and its vicinity. Philos Trans R Soc Lond B Biol Sci 300:75–106

Phalan B, Phillips RA, Silk JR, Afanasyev V and others (2007) Foraging behaviour of four albatrosses species by night and day. Mar Ecol Prog Ser 340:271–286

Qasem L, Cardew A, Wilson A, Griffiths I and others (2012) Tri-axial dynamic acceleration as a proxy for animal energy expenditure; should we be summing values or calculating the vector? PLOS ONE 7:e31187

R Core Team (2020) R: a language and environment for statistical computing. R Foundation for Statistical Computing, Vienna

Richardson PL (2011) How do albatrosses fly around the world without flapping their wings? Prog Oceanogr 88: 46–58

Richardson PL (2015) Upwind dynamic soaring of albatrosses and UAVs. Prog Oceanogr 130:146–156

Richardson PL, Wakefield ED, Phillips RA (2018) Flight speed and performance of the wandering albatross with respect to wind. Mov Ecol 6:3

Rutz C, Hays GC (2009) New frontiers in biologging science. Biol Lett 5:289–292

Sachs G (2005) Minimum shear wind strength required for dynamic soaring of albatrosses. Ibis (Lond 1859) 147: 1–10

Sachs G (2016) In-flight measurement of upwind dynamic soaring in albatrosses. Prog Oceanogr 142:47–57

Sachs G, Traugott J, Nesterova AP, Dell'Omo G and others (2012) Flying at no mechanical energy cost: disclosing the secret of wandering albatrosses. PLOS ONE 7: e41449

Sachs G, Traugott J, Nesterova AP, Bonadonna F (2013) Experimental verification of dynamic soaring in albatrosses. J Exp Biol 216:4222–4232

Sakamoto KQ, Takahashi A, Iwata T, Yamamoto T, Yamamoto M, Trathan PN (2013) Heart rate and estimated energy expenditure of flapping and gliding in black-browed albatrosses. J Exp Biol 216:3175–3182

Sato K, Sakamoto KQ, Watanuki Y, Takahashi A, Katsumata N, Bost CA, Weimerskirch H (2009) Scaling of soaring seabirds and implications for flight abilities of giant pterosaurs. PLOS ONE 4:e5400

Schoombie S (2021) Remotely sensing motion: the use of multiple biologging technologies to detect fine-scale, at-sea behaviour of breeding seabirds in a variable Southern Ocean environment. PhD dissertation, University of Cape Town

Schoombie S, Schoombie J, Brink CW, Stevens KL, Jones CW, Risi MM, Ryan PG (2019) Automated extraction of bank angles from bird-borne video footage using open-source software. J Ornithol 90:361–372

Shaffer SA, Costa DP, Weimerskirch H (2001a) Behavioural factors affecting foraging effort of breeding wandering albatrosses. J Anim Ecol 70:864–874

Shaffer SA, Weimerskirch H, Costa DP (2001b) Functional significance of sexual dimorphism in Wandering Albatrosses, *Diomedea exulans.* Funct Ecol 15:203–210

Shepard ELC, Wilson RP, Quintana F, Gómez Laich A and others (2008) Identification of animal movement patterns using tri-axial accelerometry. Endang Species Res 10: 47–60

Spear LB, Ainley DG (1997) Flight speed of seabirds in relation to wind speed and direction. Ibis (Lond 1859) 139: 234–251

Tarroux A, Weimerskirch H, Wang SH, Bromwich DH and others (2016) Flexible flight response to challenging wind conditions in a commuting Antarctic seabird: Do you catch the drift? Anim Behav 113:99–112

Tickell WLN (2000) Albatrosses. Pica Press, Mountfield

Van Walsum TA, Perna A, Bishop CM, Murn CP, Collins PM, Wilson RP, Halsey LG (2020) Exploring the relationship between flapping behaviour and accelerometer signal during ascending flight, and a new approach to calibration. Ibis (Lond 1859) 162:13–26

Wakefield ED, Phillips RA, Jason M, Akira F, Hiroyoshi H, Marshall GJ, Trathan PN (2009) Wind field and sex constrain the flight speeds of central-place foraging albatrosses. Ecol Monogr 79:663–679

Warham J (1977) Wing loadings, wing shapes, and flight capabilities of procellariiformes. NZ J Zool 4:73–83

Weimerskirch H, Wilson RP (2000) Oceanic respite for wandering albatrosses. Nature 406:955–956

Weimerskirch H, Wilson RP, Lys P (1997) Activity pattern of foraging in the wandering albatross: a marine predator with two modes of prey searching. Mar Ecol Prog Ser 151:245–254

Weimerskirch H, Guionnet T, Martin J, Shaffer SA, Costa DP (2000) Fast and fuel efficient? Optimal use of wind by flying albatrosses. Proc Biol Sci 267: 1869–1874

Weimerskirch H, Bonadonna F, Bailleul F, Mabille G, Dell'Omo G, Lipp HP (2002) GPS tracking of foraging albatrosses. Science 295:1259

Weimerskirch H, Louzao M, De Grissac S, Delord K (2012) Changes in wind pattern alter albatross distribution and life-history traits. Science 335:211–214

Weimerskirch H, Cherel Y, Delord K, Jaeger A, Patrick SC, Riotte-Lambert L (2014) Lifetime foraging patterns of the wandering albatross: life on the move! J Exp Mar Biol Ecol 450:68–78

Williams HJ, Shepard ELC, Duriez O, Lambertucci SA (2015) Can accelerometry be used to distinguish between flight types in soaring birds? Anim Biotelem 3:1–11

Williams HJ, Duriez O, Holton MD, Dell'Omo G, Wilson RP, Shepard ELC (2018) Vultures respond to challenges of near-ground thermal soaring by varying bank angle. J Exp Biol 221:jeb.174995

Williams HJ, Shepard ELC, Holton MD, Alarcón PAE, Wilson RP, Lambertucci SA (2020a) Physical limits of flight performance in the heaviest soaring bird. Proc Natl Acad Sci USA 117:17884–17890

Williams HJ, Taylor LA, Benhamou S, Bijleveld AI and others (2020b) Optimizing the use of biologgers for movement ecology research. J Anim Ecol 89:186–206

Wilmers CC, Nickel B, Bryce CM, Smith JA, Wheat RE, Yovovich V (2015) The golden age of bio-logging: how animal-borne sensors are advancing the frontiers of ecology. Ecology 96:1741–1753

Wood S (2011) Fast stable restricted maximum likelihood and marginal likelihood estimation of semiparametric generalized linear models. J R Stat Soc B 73:3–36

Yonehara Y, Goto Y, Yoda K, Watanuki Y and others (2016) Flight paths of seabirds soaring over the ocean surface enable measurement of fine-scale wind speed and direction. Proc Natl Acad Sci USA 113:9039–9044

Appendix.

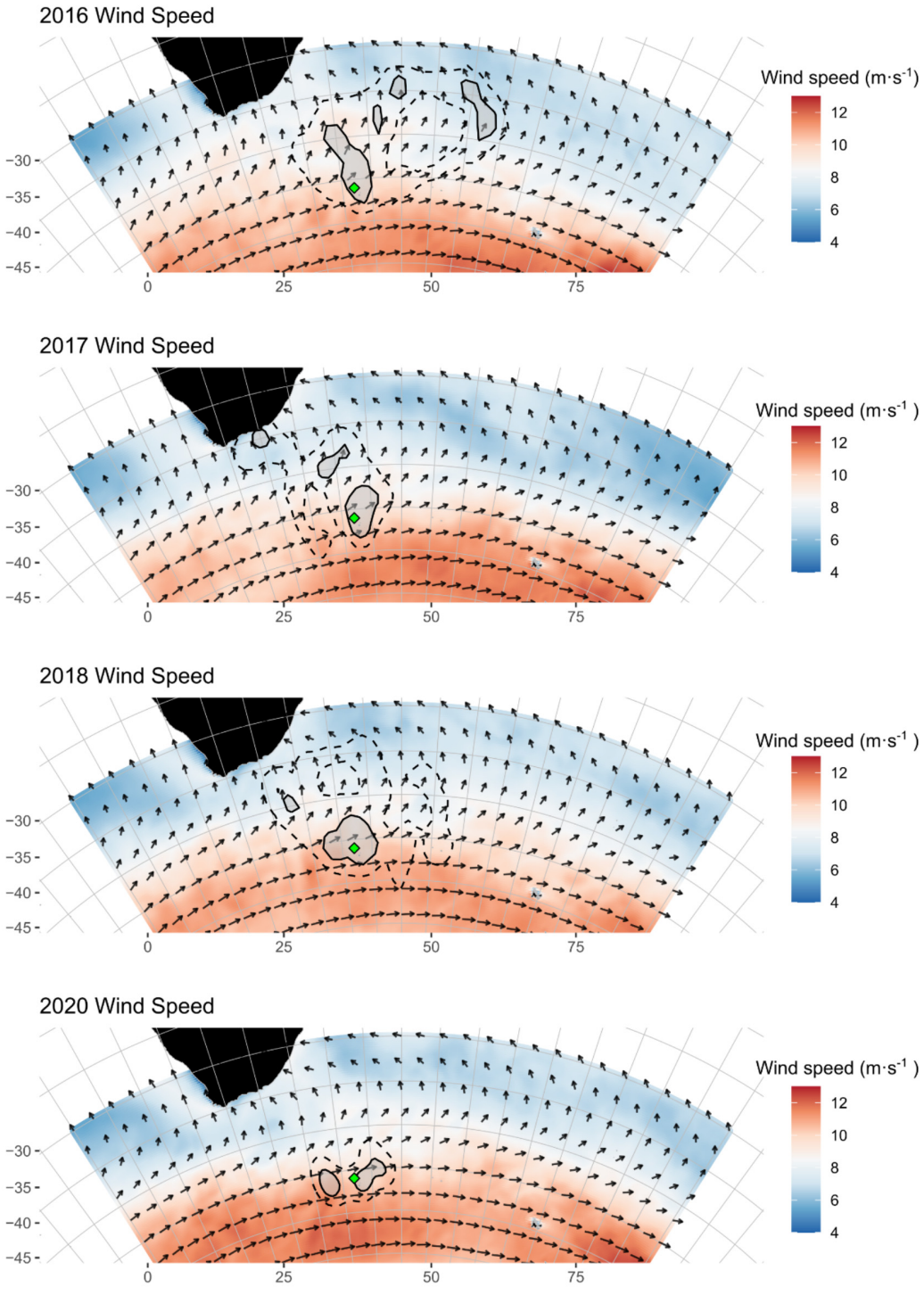

Fig. A1. Average wind speed and direction across the study period with 50% (solid line) and 90% (dashed line) kernel density estimates of track points corresponding to IMU data

Editorial responsibility: Lesley H. Thorne (Guest Editor), Stony Brook, New York, USA
Reviewed by: 2 anonymous referees

Submitted: October 18, 2022
Accepted: February 13, 2023
Proofs received from author(s): April 5, 2023